Ocean-atmosphere interactions modulate irrigation's climate impacts

Nir Y Krakauer[1], Michael J Puma[2,3,4], Benjamin I Cook[3], Pierre Gentine[5], and Larissa Nazarenko[2,3]

[1]Department of Civil Engineering and NOAA-CREST, The City College of New York, New York, NY, 10031, USA
[2]Center for Climate Systems Research, Columbia University, New York, NY 10025, USA
[3]NASA Goddard Institute for Space Studies, New York, NY 10025, USA
[4]Center for Climate and Life, Columbia University, Palisades, NY 10964, USA
[5]Earth and Environmental Engineering, School of Engineering and Applied Science, Columbia University, New York, New York, USA

Correspondence to: NY Krakauer (nkrakauer@ccny.cuny.edu)

Abstract. Numerous studies have focused on the local and regional climate effects of irrigated agriculture and other land cover and land use change (LCLUC) phenomena, but there are few studies on the role of ocean-atmosphere interaction in modulating irrigation climate impacts. Here, we compare simulations of the equilibrium effect of contemporary irrigation geographic extent and intensity on climate with and without interactive sea surface temperatures. We find that ocean-atmosphere interaction

5 does impact the magnitude of global-mean and spatially varying climate impacts, greatly increasing their global reach. The interaction amplifies irrigation-driven standing wave patterns in the tropics and midlatitudes in our simulations, approximately doubling the global mean amplitude of surface temperature changes due to irrigation. Subject to confirmation with other models, these findings imply that LCLUC is an important contributor to climate change even in remote areas such as the Southern Ocean. Attribution studies should include interactive oceans and need to consider LCLUC, including irrigation, as a

10 truly global forcing that affects climate and the water cycle over ocean as well as land areas.

1 Introduction

Anthropogenic land cover and land use change (LCLUC) affects climate by modifying water, sensible heat, and radiation fluxes at the land surface (Chase et al., 2000; Gordon et al., 2005; Brovkin et al., 2006; Findell et al., 2007; Krakauer et al., 2010; Mahmood et al., 2014). One important mode of LCLUC has been the dramatic expansion in irrigated agriculture over

15 the past century. Resultant local climate changes, notably growing-season daytime cooling resulting primarily from increased evapotranspiration, have been diagnosed from observations (Bonfils and Lobell, 2007; Lobell and Bonfils, 2008; Misra et al., 2012). Remote (non-local) impacts of irrigation are less well constrained. Global climate models (GCMs) can be run with and without an irrigation scheme to assess local climate effects as well as remote impacts (such as downwind enhancement of precipitation), which would be difficult to deduce with confidence from observations alone (Lo et al., 2013; Alter et al., 2015).

20 Many GCM studies of irrigation's climate impacts have been conducted with prescribed sea surface temperatures (SSTs) (Boucher et al., 2004; Puma and Cook, 2010; Lo and Famiglietti, 2013; de Vrese et al., 2016), while several did include

ocean-atmosphere interaction (Lobell et al., 2006; Cook et al., 2011, 2015). Various studies have highlighted the importance of interactive atmosphere-ocean coupling for accurately reproducing various phenomena in GCMs. These include Indian monsoon rainfall (Kumar et al., 2005; Wu and Kirtman, 2004; Shukla et al., 2014) and the relationship between sea level pressure and SST trends (Copsey et al., 2006; Meng et al., 2012). Further, oceans may be important for amplifying responses from LCLUC

5 forcings, providing an additional source of memory that can allow anomalies to persist and carry over between seasons. For example, studies of afforestation and deforestation at high Northern latitudes (Bonan et al., 1992; Swann et al., 2010) show that responses to these LCLUC forcings are amplified in simulations that included interactive SSTs. To date, however, no studies have explicitly investigated the effect of interactive versus prescribed SSTs on model responses to realistic irrigation forcing.

In this study, therefore, we investigate the possible role of atmosphere-ocean interaction in modulating the irrigation climate

10 forcing. We conduct GCM simulations of steady-state climate with and without present-day irrigation extents and with either prescribed SSTs or a thermodynamic slab ocean model.

2 Methods

2.1 Model runs

We analyze several different model experiments to investigate irrigation forcing of climate, all using the GCM ModelE2 ($2° \times$

15 $2.5°$ latitude/longitude resolution), the latest version of the GISS atmosphere general circulation model with 40 vertical layers in the atmosphere and updated physics (Schmidt et al., 2014). Irrigation water is added to the vegetated fraction of the grid cell at the top of the soil column, beneath the vegetation canopy. Irrigation rates are nominally for the year 2000, taken from a global gridded reconstruction (Wisser et al., 2010) (Figure 1). Water for irrigation is initially withdrawn from rivers and lakes in the same grid cell. If irrigation demand is not satisfied by these surface sources, water is added under the assumption that

20 it is taken from groundwater sources that are not represented in the model (i.e., 'fossil' groundwater). The irrigation rate is kept constant over the course of the day and applied for every sub-daily time step. Irrigation water will either infiltrate the soil column or runoff to the streams in the grid cell. The total amount of irrigation water summed to 0.019 mm per day (6.8 mm per year) globally, with a mean of 0.46 mm per day (168 mm per year) over irrigated land grid cells (defined as those for which the average irrigation amount was at least 0.1 mm per day). Additional details and discussion of the irrigation scheme are in Puma

25 and Cook (2010) and Cook et al. (2011). As opposed to 'Irrigation' (irrig) runs, in 'Control' (ctrl) runs no irrigation water was applied.

Irrigation and Control simulations were carried out with two different ocean configurations. The simplest involves forcing the atmosphere model with prescribed monthly sea surface temperatures (SSTs) and sea ice. Average SSTs and sea ice values are computed based on 1996 to 2004 data using the Hadley Center analysis (Rayner et al., 2003). We refer to this as the

30 atmosphere-only, fixed-SST, or A configuration. In the second configuration (referred to as 'q-flux' mode, interactive-SST, interactive-(surface)-ocean, or O configuration), the ocean is represented as a 65-m deep mixed layer, with a prescribed internal heat source to represent the effects of horizontal and vertical ocean mixing and advection.
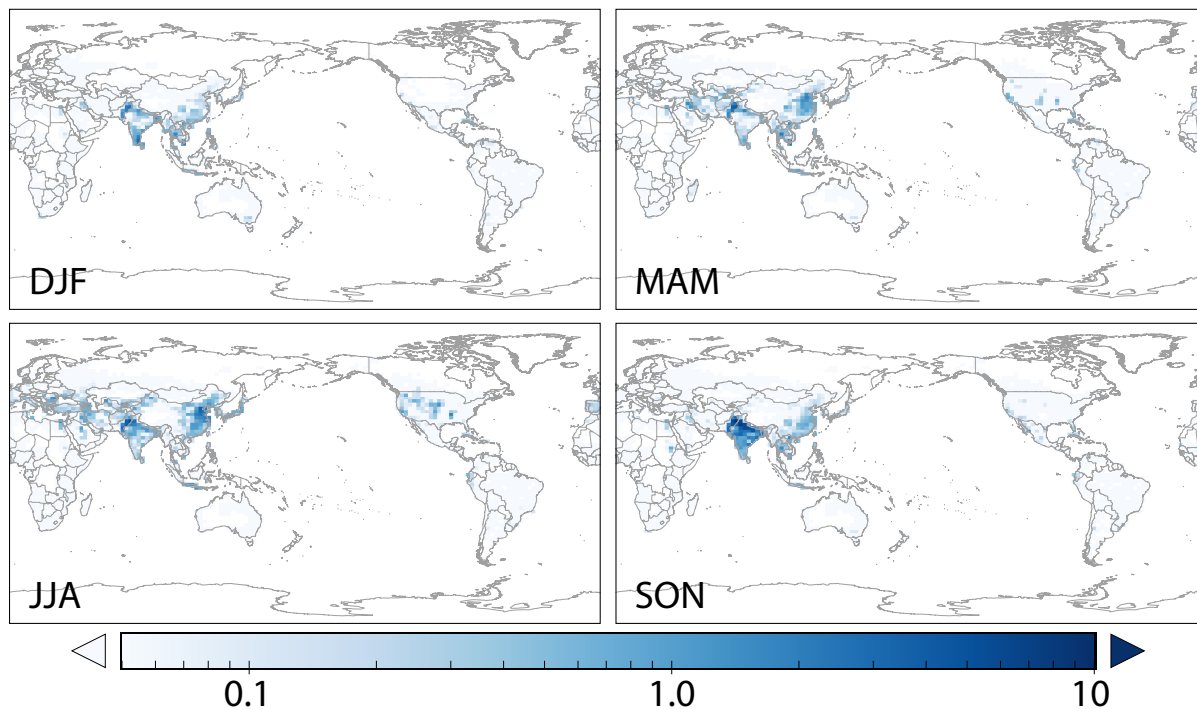
Figure 1. Applied irrigation by season (mm per day). The scale is logarithmic.

The four simulations – irrig-A, ctrl-A, irrig-O, ctrl-O – were run 60 years each. The q-flux mode takes approximately 10 years to reach equilibrium under constant forcings, so we analyzed only the last 50 years of each simulation.

2.2 Analysis of differences between runs

For climate variables of interest, we considered irrig-ctrl differences in the monthly fields for both the A and O configurations. The irrig-ctrl difference field for the A set of experiments is referred to as Δ_A, and the irrig-ctrl difference field for the O set of experiments is referred to as Δ_O. The impact of interactive SST on the equilibrium irrig-ctrl difference was then obtained as $\Delta\Delta \equiv \Delta_O - \Delta_A$.

The significance of $\Delta_A, \Delta_O, \Delta\Delta$, either at individual grid points or spatially averaged, was estimated using Student's t-test on their time series over the 50-year analysis period, with the degrees of freedom adjusted based on the lag-1 autocorrelation of the time series. As metrics of overall irrigation and ocean configuration impacts, we looked at the mean and the root mean square (rms) of $\Delta_A, \Delta_O, \Delta\Delta$ aggregated globally over irrigated areas (which we defined as grid cells and months where the applied irrigation was over 0.1 mm day^{-1}); non-irrigated land areas; and ocean areas. We considered annual means of these quantities as well as seasonal means. For seasonal means, aggregation was performed only over the zone of the Northern

Hemisphere where the vast majority of the irrigation takes place (8°-46°N, 92% of global irrigation), to preserve consistent seasonality.

15   We focus on climate variables that quantify directly conditions and moisture status at the earth surface (surface air temperature, SST [only over ocean], precipitation, soil moisture [only over land], cloud fraction); terms in the surface energy balance that are affected by irrigation (latent and sensible heat fluxes); and circulation-related quantities (sea-level pressure and geopotential height fields) that can provide insight into how irrigation effects on surface energy and water balance could propagate to impact climate in distant regions.

3   Results

3.1   Impact of interactive SST on spatial-mean irrigation responses

Irrigation-induced surface air cooling, though still concentrated over the irrigated areas, spread over ocean areas in the interactive-SST simulation. Global-mean above-ocean surface air temperatures decreased 0.08 K and sea surface temperatures decreased 0.07 K (Table 1). In the fixed-SST irrigation simulation, precipitation slightly decreased over the irrigated areas and increased elsewhere. Compared to the fixed-SST irrigation simulation, the cooling over the oceans slightly reduced evaporation and precipitation in the interactive-SST simulation. Interactive SST did not significantly modify the global mean enhancements in soil moisture and cloudiness due to irrigation (Table 1). Irrigation-induced evaporative and sensible surface heating were both slightly diminished in the interactive-SST simulation, consistent with the cooler surface temperatures and reduced precipitation (Table 1). As expected, the mean atmospheric pressure responded inversely to the temperature change, with higher pressure in the irrigated areas (consistent with the reduced precipitation there). The mean 300-mb height decreased significantly more in the interactive-SST simulation even in the irrigated areas, showing that, compared to fixed SST, interactive SST spreads the cooling due to irrigation throughout the atmospheric column (Table 1).

Table 2 shows changes by season (averaged over 8°-46°N) for surface air temperature. Over land, cooling is greatest in the summer and fall, when the largest amount of irrigation water is applied, and the mean amount is not significantly affected by whether SST is interactive. Over ocean, cooling is more uniform across seasons, and is much greater in the interactive SST simulation (Table 2).

3.2   Impact of interactive SST on spatial variability of irrigation responses

The global or zonal mean impacts just shown conceal much spatial variability in the response to irrigation, which is best depicted in maps. The rms of the spatial field of irrigation response for the same climate variables shows that interactive SST tends to increase this spatial variability over the ocean and non-irrigated land, even for variables such as over-ocean cloud cover for which the mean response is not significantly affected, implying that interactive SST on the whole enhances non-local irrigation impacts on climate. One exception is that interactive SST decreases the spatial variability in latent and sensible heat

Table 1. Mean impact of irrigation on climate quantities with and without interactive sea surface temperatures.

	Irrigated land				Non-irrigated land				Ocean			
	Mean	Δ_A	Δ_O		Mean	Δ_A	Δ_O		Mean	Δ_A	Δ_O	
Surface air temperature (°C)	18.764	-0.665	-0.697	-	7.760	-0.078	-0.123	-	16.008	-0.003	-0.084	***
Sea surface temperature (°C)									21.676	0	-0.0674	***
Precipitation (mm d^{-1})	3.085	-0.032	-0.082	-	1.935	0.032	0.036	-	3.371	0.011	0.005	*
Soil moisture (mm)	462.7	60.5	56.6	-	416.0	7.2	9.7	-				
Cloud cover (%)	50.27	1.28	0.96	-	59.13	0.43	0.33	-	63.37	0.07	0.09	-
Latent heat (W m^{-2})	55.56	9.08	8.38	***	39.07	0.63	0.51	-	104.93	0.03	-0.08	*
Sensible heat (W m^{-2})	-47.99	6.03	5.49	**	-38.35	0.48	0.44	-	-18.80	0.05	-0.03	***
Sea-level pressure (mb)	1010.36	0.47	0.39	-	1010.16	0.11	0.02	-	1009.89	-0.05	0.01	**
300-mb height (m)	9459.55	-1.90	-4.58	**	9207.85	-0.11	-3.11	***	9316.66	-0.05	-1.76	***

Means are for the ctrl-A (no irrigation, fixed SST) simulation. Significance level (two-tailed) of differences due to interactive sea surface temperature: -not significant ($p > 0.05$), *0.05, **0.01, ***0.001.

Table 2. Mean impact of irrigation on seasonal surface air temperature (°C) with and without interactive sea surface temperatures.

	Irrigated land				Non-irrigated land				Ocean			
	Mean	Δ_A	Δ_O		Mean	Δ_A	Δ_O		Mean	Δ_A	Δ_O	
Winter (DJF)	10.407	-0.606	-0.633	-	10.302	-0.036	-0.130	-	19.282	0.000	-0.188	***
Spring (MMA)	19.414	-0.622	-0.663	-	18.530	-0.118	-0.165	-	20.522	-0.021	-0.170	***
Summer (JJA)	26.242	-0.674	-0.726	-	26.333	-0.329	-0.396	-	24.432	-0.030	-0.178	***
Fall (SON)	19.474	-0.885	-0.891	-	19.580	-0.225	-0.307	-	23.487	-0.020	-0.163	***

Means are for the ctrl-A (no irrigation, fixed SST) simulation. Significance level (two-tailed) of differences due to interactive sea surface temperature: -not significant ($p > 0.05$), *0.05, **0.01, ***0.001.

Table 3. Root mean square impact of irrigation on climate quantities with and without interactive sea surface temperatures.

	Irrigated land			Non-irrigated land			Ocean		
	Δ_A	Δ_O		Δ_A	Δ_O		Δ_A	Δ_O	
Surface air temperature (°C)	1.289	1.267	-	0.989	1.047	*	0.374	0.769	***
Sea surface temperature (°C)							0	0.549	***
Precipitation (mm d^{-1})	0.985	0.977	-	0.547	0.590	**	0.847	0.916	***
Soil moisture (mm)	120.6	119.0	-	52.9	59.0	***			
Cloud cover (%)	4.64	4.72	-	4.01	4.10	-	3.07	3.46	***
Latent heat (W m^{-2})	17.31	17.01	*	5.90	6.19	*	7.96	7.55	***
Sensible heat (W m^{-2})	12.14	11.94	-	6.22	6.58	**	3.55	3.40	*
Sea-level pressure (mb)	1.01	0.97	-	1.66	1.47	-	1.45	1.40	-
300-mb height (m)	17.31	17.68	-	25.72	24.93	-	22.27	23.84	*

Significance level (two-tailed) of differences due to interactive sea surface temperature: -not significant ($p > 0.05$), *0.05, **0.01, ***0.001.

irrigation responses over the ocean, presumably because in those simulations SST can adjust to changes in air temperature in a way that reduces the equilibrium change in surface fluxes (Table 3).

30   We show illustrative maps of the seasonal-mean irrigation response with and without interactive SST (Δ_A, Δ_O). Under fixed SST, irrigation-induced changes in surface air temperature (Figure 2) are primarily local to major irrigation regions such as India, China, and the USA, and effects in the ocean tend to be small, except in the North Pacific. Under interactive SST, irrigation-induced regional changes tend to have larger amplitude ($\sim$0.8 compared to $\sim$0.4 K) and are also found in the tropical and southern oceans. Under fixed SST in Boreal winter, the middle and high northern latitudes show a stationary wave pattern of alternating warm and cool anomalies due to irrigation (which during that season is concentrated in the Indian subcontinent).

5   Under interactive SST, these Boreal winter anomalies shift locations somewhat (for example, the cooling centered in the eastern USA under fixed SST is attenuated) and persist to a greater extent during the other seasons, and analogous wave patterns are also seen in the Southern Ocean and Antarctica. Under interactive SST, surface air temperature anomalies outside irrigated areas tend to be closely associated with SST anomalies of the same sign (Figure 3), which provide a mechanism for the surface air temperature anomalies to persist across seasons.

10   Under fixed SST, a reduction in 300-mb height (Figure 4) (corresponding to cooling of the atmospheric column) is seen primarily around irrigation regions in the northern midlatitudes, while under interactive SST the reduction in the northern mid-latitudes is more zonally uniform, and there is also a stationary wave pattern in the Southern Hemisphere roughly corresponding to locations of surface air temperature changes there. Over the oceans, irrigation-induced SST changes in the interactive-SST simulations are similar to surface air temperature changes (with some larger changes in the Arctic and Antarctic margins due

to shifts in sea ice distribution; Figure 3), supporting the role of air-sea interaction in driving the divergence in surface air temperature and geopotential height irrigation responses between the fixed-SST and interactive-SST simulations. Particularly in Boreal winter, the same stationary wave pattern seen for temperature is found in the upper atmosphere, with shifted phase under interactive SST compared to fixed SST (Figure 4). Precipitation impacts (Figure 5) are strongest over the tropics and subtropics and reflect, for example, a northward shift due to irrigation in the intertropical convergence zone in and south of India in Boreal winter and a southward shift in Boreal summer. Latent heat impacts (Figure 6) reflect both increased evapotranspiration where there is irrigation and the impacts of nonlocal changes in temperature and precipitation, e.g. less evaporation over western Australia in Austral summer associated with reduced precipitation there due to irrigation under interactive SSTs.

The role of interactive SST in non-local irrigation climate forcing can be seen, for example, for precipitation in eastern Africa. de Vrese et al. (2016) performed a modeling study using different atmosphere and land surface models than we utilized, and found that with fixed SST, irrigation, specifically over Asia, results in moisture transport and precipitation increases over eastern Africa in boreal spring. We see the same effect in MAM for our fixed-SST runs (Δ_A in Figure 5), supporting the robustness across atmosphere and land surface models of the non-local precipitation impacts of irrigation found by de Vrese et al. (2016). However, the interactive-SST runs (Δ_O in Figure 5) show less pronounced (and mostly statistically non-significant) precipitation responses due to irrigation over the same regions and season, as the precipitation enhancement moves further south and east. Moreover, with interactive SST a precipitation increase for the southern Horn of Africa remains during boreal summer and is enhanced during boreal winter. Thus, ocean-atmosphere interactions may importantly affect the magnitude and location of non-local irrigation impacts on climate, such as those potentially implicated in precipitation trends in eastern Africa.

4 Discussion

The current work suggests that an interactive-SST (q-flux) model configuration, compared to one with fixed SSTs, results in similar mean local climate effects in the irrigated regions, but generally larger non-local effects, particularly over the oceans. In response to the application of realistic present-day irrigation amounts, the q-flux configuration generates stationary wave patterns across a range of latitudes in climate variables such as surface air temperature, SST, and geopotential height. These wave patterns have fairly large amplitudes (e.g. up to ∼1 K in SST, similar to the magnitude of anthropogenic warming impacts over the past century). The stationary waves generated are qualitatively similar to those previously studied as occurring in response to zonal asymmetries (Held et al., 2002; Shaman and Tziperman, 2005). A recent atmosphere-only GCM study (Koster et al., 2014) identified phase locking and amplification of a planetary wave as a potential mechanism for nonlocal climate impacts of soil moisture changes (such as those imposed by irrigation) in Boreal spring and summer, but did not attempt to assess to what extent such feedbacks are likely to be affected by air-sea interactions. In our simulations, these patterns are less widespread when SST is fixed, implying that air-sea interaction is key to their propagation and persistence across seasons.
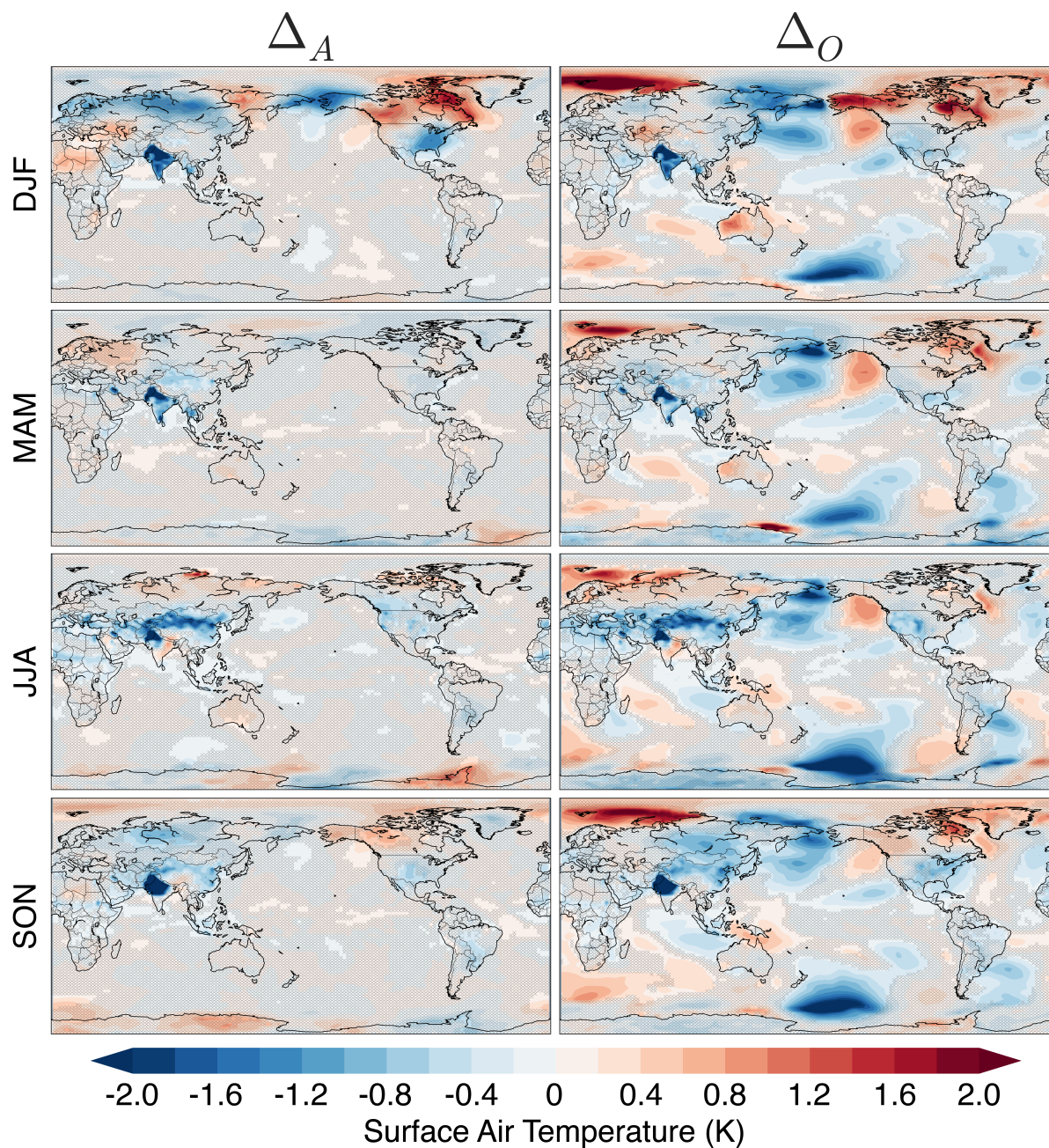
Figure 2. (Difference in surface air temperature (K) by season due to irrigation with fixed SST (Δ_A) and with interactive SST (Δ_O).
Differences not significant at the 0.05 level are hatched gray.
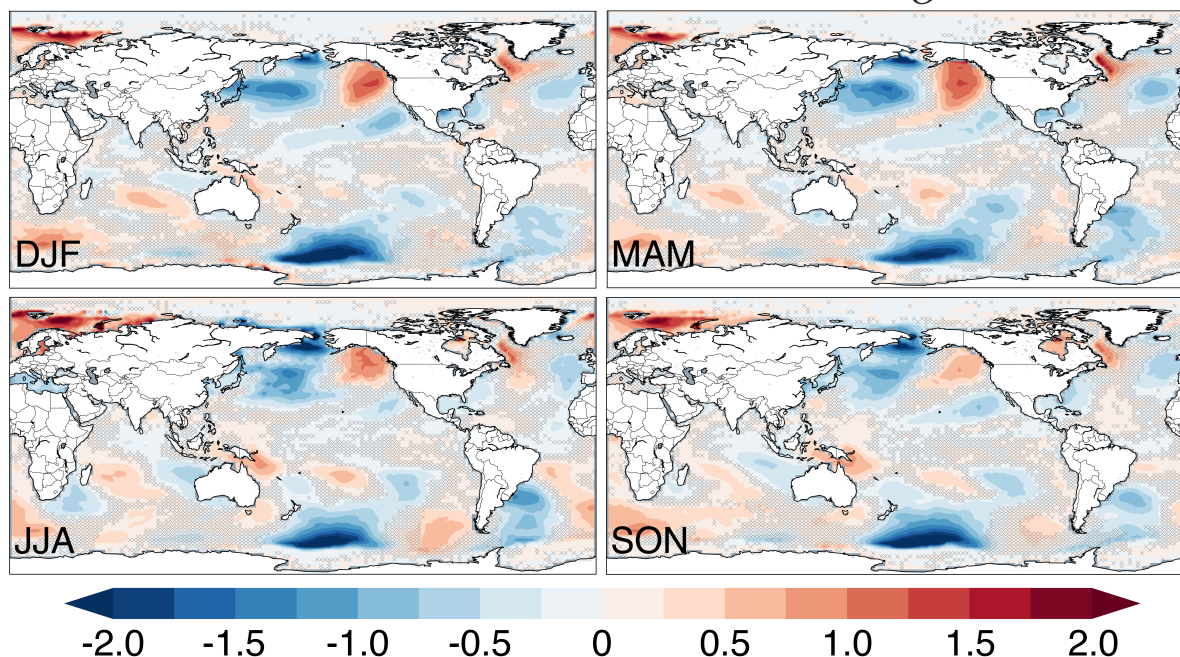
Figure 3. Difference in SST (K) due to irrigation with interactive SST (Δ_O).

While comparison with such past studies suggests that the occurrence of stationary waves amplified by air-sea interaction in response to irrigation is likely robust, their location and magnitude may be sensitive to, for example, aspects of our atmosphere model parametrization, background climate and ocean fluxes, and details of how the irrigation is applied. Systematic multi-model intercomparisons of responses to irrigation and other LCLUC forcings could aid in understanding these sensitivities, illuminate the physical mechanisms at play, and identify suitable targets for testing modeled LCLUC-induced non-local climate change against observations.

Our q-flux simulations gave an equilibrium impact of irrigation forcing on climate. Simulated changes with interactive SST are more plausible than those simulated under fixed SST in that energy is being conserved (within the constraints of the q-flux surface ocean framework). However, in reality, ocean circulation and mixing delay equilibrium with forcings such as irrigation. Since irrigation has only been practiced globally at its current magnitude for the past few decades, it is expected that transient changes in SST due to irrigation for the current climate system would be smaller than the equilibrium changes simulated here, though nonlinear effects on ocean circulation could possibly also enhance climate impacts compared to our q-flux configuration (which had effectively constant ocean heat transport). Preliminary comparison of SSTs in irrigation and no-irrigation runs of GISS ModelE2 with time-varying forcings and a three-dimensional dynamic ocean model (Cook et al., 2015) suggests that around the year 2000, the amplitude of non-local SST changes due to irrigation might have been ∼0.1-0.2 K, instead of the
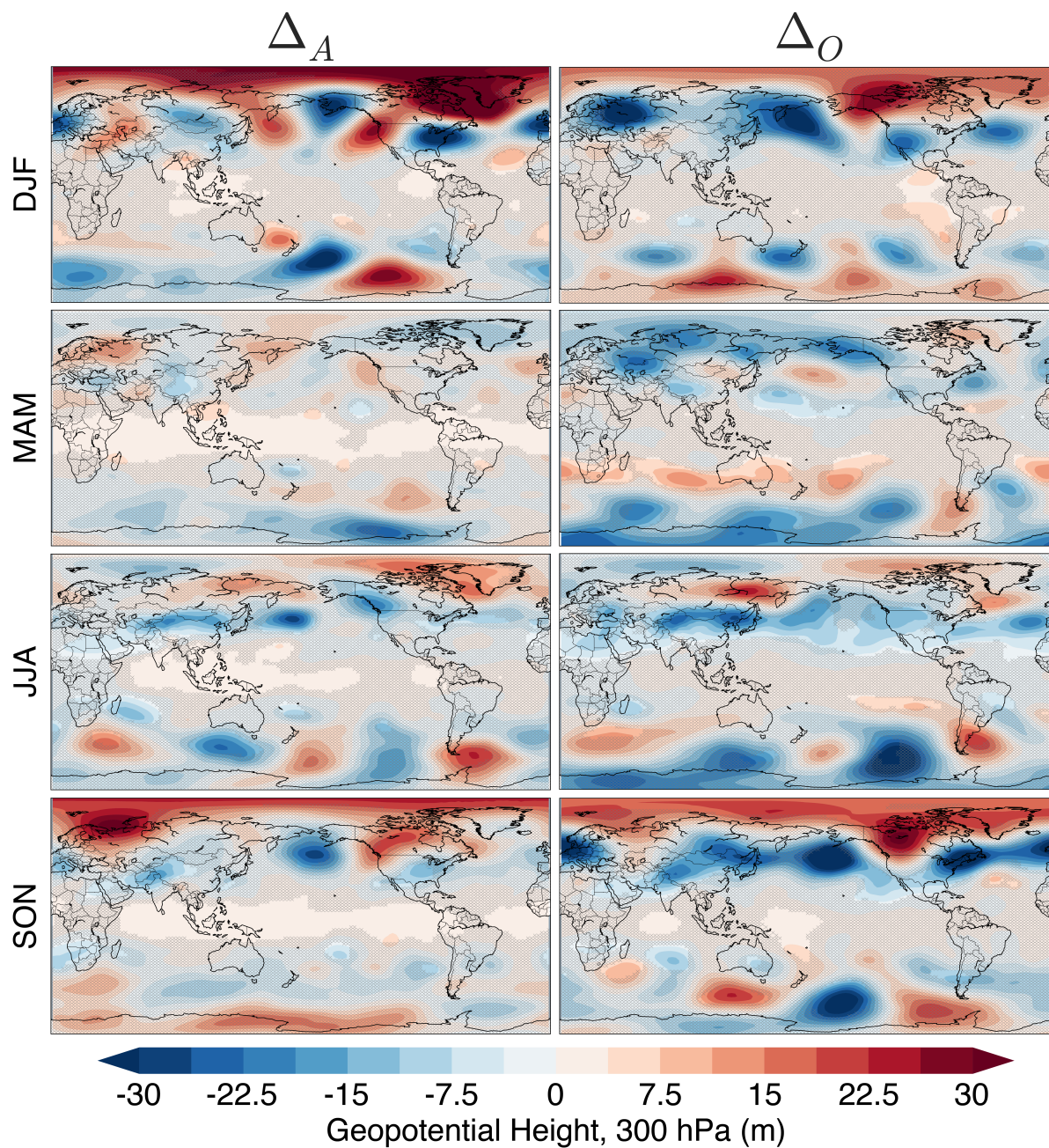
Figure 4. Same as Figure 2, but for 300-mb height differences (m).

~0.5-1 K seen here with a q-flux model run to equilibrium. These differences between transient and equilibrium responses to LCLUC in the coupled atmosphere-ocean system should be explored in more detail. In fact, future changes in irrigation are
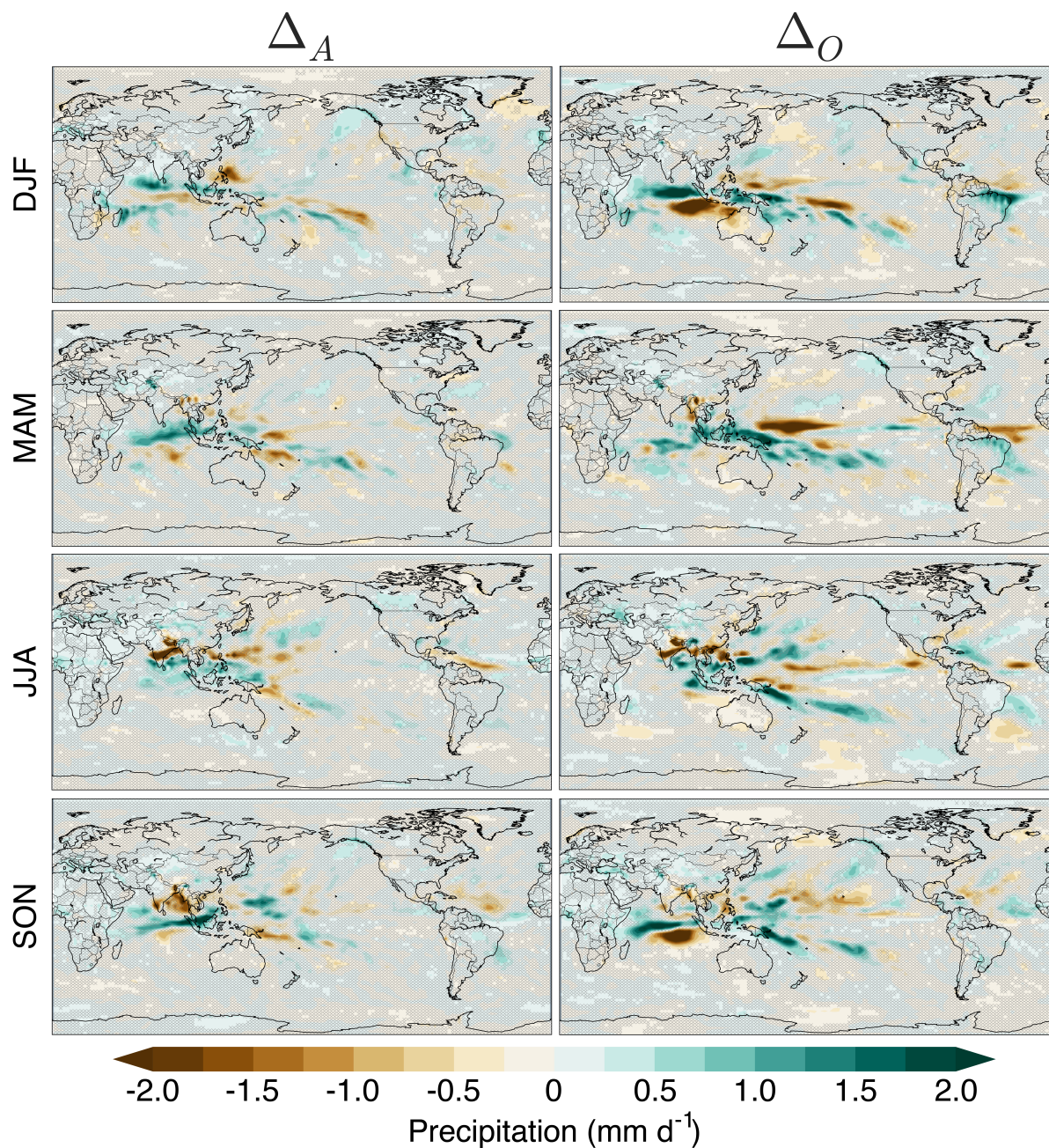
Figure 5. Same as Figure 2, but for precipitation differences (mm/day).

highly uncertain (Wada et al., 2013; Elliott et al., 2014), particularly given the depletion of groundwater sources of irrigation water in many major agricultural areas (Gleeson et al., 2012; Krakauer et al., 2013; Leng et al., 2014). Despite these limitations,
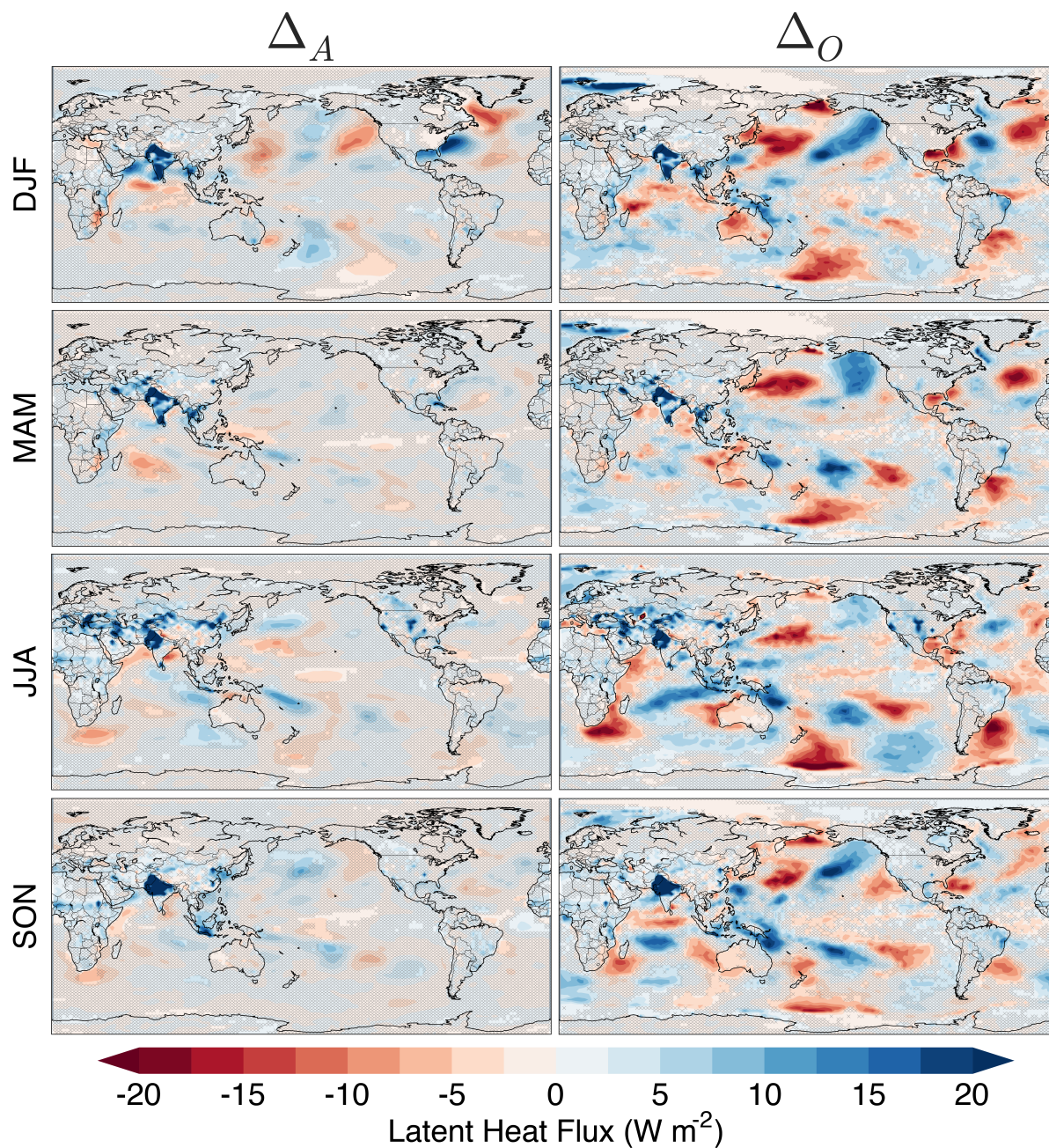
Figure 6. Same as Figure 2, but for surface latent heat flux differences (W m^{-2}).

our work illustrates that studies of irrigation climate impacts that use either global models with fixed SST configurations or

regional models with fixed boundary conditions (Im et al., 2014; Alter et al., 2015) may miss some of the impact of irrigation on non-local climate.

5 Conclusions

We compared simulations of the equilibrium effect of contemporary irrigation extent on climate with and without interactive sea surface temperatures to show that air-sea interaction does impact the magnitude of global-mean and spatially-varying climate impacts and greatly increase their global reach. In these simulations, air-sea interaction amplified irrigation-driven standing wave patterns in the tropics and midlatitudes, approximately doubling the global mean amplitude of surface temperature changes due to irrigation. Subject to confirmation with other models and consideration of irrigation's time evolution, these

5   findings imply that LCLUC may be an important contributor to climate change even in remote areas such as the Southern Ocean, and that attribution studies need to consider LCLUC such as irrigation as truly global forcings that affect climate and the water cycle in ocean as well as land areas.

Code and data availability

The GISS GCM source code can be accessed from http://www.giss.nasa.gov/tools/modelE/ for free download and use. Docu-

10   mentation of model configurations and further references are also available there.

Acknowledgements. Climate modeling at GISS is supported by the NASA Modeling, Analysis, and Prediction program. Resources supporting this work were provided by the NASA High-End Computing (HEC) Program through the NASA Center for Climate Simulations (NCCS) at Goddard Space Flight Center. The authors specifically thank Maxwell Kelly for assistance with the model irrigation module and output diagnostics. M.J. Puma gratefully acknowledges support from the Interdisciplinary Global Change Research under NASA cooperative

15   agreement NNX14AB99A supported by the NASA Climate and Earth Observing Program and from the Columbia University Center for Climate and Life, where he is a Climate and Life Fellow. NYK gratefully acknowledges support from NOAA under grants NA11SEC4810004, NA12OAR4310084, and NA15OAR4310080; from CUNY through PSC-CUNY Award 68346-00 46 and CUNY CIRG Award 2207; and from USAID IPM Innovation Lab award "Participatory Biodiversity and Climate Change Assessment for Integrated Pest Management in the Annapurna-Chitwan Landscape, Nepal". All statements made are the views of the authors and not the opinions of the funding agency or the U.S. government.

References

Alter, R. E., Im, E.-S., and Eltahir, E. A. B.: Rainfall consistently enhanced around the Gezira Scheme in East Africa due to irrigation, Nature Geoscience, 8, 763–767, doi:10.1038/ngeo2514, 2015.

5 Bonan, G. B., Pollard, D., and Thompson, S. L.: Effects of boreal forest vegetation on global climate, Nature, 359, 716–718, doi:10.1038/359716a0, 1992.

Bonfils, C. and Lobell, D.: Empirical evidence for a recent slowdown in irrigation-induced cooling, Proceedings of the National Academy of Sciences, 104, 13 582–13 587, doi:10.1073/pnas.0700144104, 2007.

Boucher, O., Myhre, G., and Myhre, A.: Direct human influence of irrigation on atmospheric water vapour and climate, Climate Dynamics, 10 22, 597–603, doi:10.1007/s00382-004-0402-4, 2004.

Brovkin, V., Claussen, M., Driesschaert, E., Fichefet, T., Kicklighter, D., Loutre, M. F., Matthews, H. D., Ramankutty, N., Schaeffer, M., and Sokolov, A.: Biogeophysical effects of historical land cover changes simulated by six Earth system models of intermediate complexity, Climate Dynamics, 26, 587–600, doi:10.1007/s00382-005-0092-6, http://www.springerlink.com/content/x7v04082qk07l5t0/, 2006.

Chase, T. N., Sr., R. A. P., Kittel, T. G. F., Nemani, R. R., and Running, S. W.: Simulated impacts of historical land cover changes on global 15 climate in northern winter, Climate Dynamics, 16, 93–105, doi:10.1007/s003820050007, 2000.

Cook, B. I., Puma, M. J., and Krakauer, N. Y.: Irrigation induced surface cooling in the context of modern and increased greenhouse gas forcing, Climate Dynamics, 37, 1587–1600, doi:10.1007/s00382-010-0932-x, 2011.

Cook, B. I., Shukla, S. P., Puma, M. J., and Nazarenko, L. S.: Irrigation as an historical climate forcing, Climate Dynamics, 44, 1715–1730, doi:10.1007/s00382-014-2204-7, 2015.

20 Copsey, D., Sutton, R., and Knight, J. R.: Recent trends in sea level pressure in the Indian Ocean region, Geophysical Research Letters, 33, L19 712, doi:10.1029/2006GL027175, 2006.

de Vrese, P., Hagemann, S., and Claussen, M.: Asian Irrigation, African Rain: Remote Impacts of Irrigation, Geophysical Research Letters, pp. n/a–n/a, doi:10.1002/2016GL068146, http://dx.doi.org/10.1002/2016GL068146, 2016.

Elliott, J., Deryng, D., Müller, C., Frieler, K., Konzmann, M., Gerten, D., Glotter, M., Flörke, M., Wada, Y., Best, N., et al.: Constraints and 25 potentials of future irrigation water availability on agricultural production under climate change, Proceedings of the National Academy of Sciences, 111, 3239–3244, 2014.

Findell, K. L., Shevliakova, E., Milly, P. C. D., and Stouffer, R. J.: Modeled impact of anthropogenic land cover change on climate, Journal of Climate, 20, 3621–3634, doi:10.1175/JCLI4185.1, 2007.

Gleeson, T., Wada, Y., Bierkens, M. F. P., and van Beek, L. P. H.: Water balance of global aquifers revealed by groundwater footprint, Nature, 30 488, 197–200, doi:10.1038/nature11295, 2012.

Gordon, L. J., Steffen, W., Jonsson, B. F., Folke, C., Falkenmark, M., and Johannessen, A.: Human modification of global water vapor flows from the land surface, Proceedings of the National Academy of Sciences, 102, 7612–7617, doi:10.1073/pnas.0500208102, 2005.

Held, I. M., Ting, M., and Wang, H.: Northern winter stationary waves: theory and modeling, Journal of Climate, 15, 2125–2144, doi:10.1175/1520-0442(2002)015<2125:NWSWTA>2.0.CO;2, 2002.

35 Im, E.-S., Marcella, M. P., and Eltahir, E. A. B.: Impact of potential large-scale irrigation on the West African monsoon and its dependence on location of irrigated area, Journal of Climate, 27, 994–1009, doi:10.1175/JCLI-D-13-00290.1, 2014.

Koster, R. D., Chang, Y., and Schubert, S. D.: A mechanism for land-atmosphere feedback involving planetary wave structures, Journal of Climate, 27, 9290–9301, doi:10.1175/JCLI-D-14-00315.1, 2014.

Krakauer, N. Y., Cook, B. I., and Puma, M. J.: Contribution of soil moisture feedback to hydroclimatic variability, Hydrology and Earth System Sciences, 14, 505–520, doi:http://www.hydrol-earth-syst-sci.net/14/505/2010/, 2010.

Krakauer, N. Y., Puma, M. J., and Cook, B. I.: Impacts of soil-aquifer heat and water fluxes on simulated global climate, Hydrology and Earth System Sciences, 17, 1963–1974, doi:10.5194/hess-17-1963-2013, 2013.

Kumar, K. K., Hoerling, M., and Rajagopalan, B.: Advancing dynamical prediction of Indian monsoon rainfall, Geophysical Research Letters, 32, L08 704, doi:10.1029/2004GL021979, 2005.

Leng, G., Huang, M., Tang, Q., Gao, H., and Leung, L. R.: Modeling the effects of groundwater-fed irrigation on terrestrial hydrology over the conterminous United States, Journal of Hydrometeorology, 15, 957–972, doi:10.1175/JHM-D-13-049.1, 2014.

Lo, M.-H. and Famiglietti, J. S.: Irrigation in California's Central Valley strengthens the southwestern U. S. water cycle, Geophysical Research Letters, doi:10.1002/grl.50108, 2013.

Lo, M.-H., Wu, C.-M., Ma, H.-Y., and Famiglietti, J. S.: The response of coastal stratocumulus clouds to agricultural irrigation in California, Journal of Geophysical Research, 118, 6044–6051, doi:10.1002/jgrd.50516, 2013.

Lobell, D. B. and Bonfils, C.: The Effect of Irrigation on Regional Temperatures: A Spatial and Temporal Analysis of Trends in California, 1934-2002, Journal of Climate, 21, 2063–2071, doi:10.1175/2007JCLI1755.1, 2008.

Lobell, D. B., Bala, G., Bonfils, C., and Duffy, P. B.: Potential bias of model projected greenhouse warming in irrigated regions, Geophysical Research Letters, 33, L13 709, doi:10.1029/2006GL026770, 2006.

Mahmood, R., Pielke, R. A., Hubbard, K. G., Niyogi, D., Dirmeyer, P. A., McAlpine, C., Carleton, A. M., Hale, R., Gameda, S., Beltrán-Przekurat, A., Baker, B., McNider, R., Legates, D. R., Shepherd, M., Du, J., Blanken, P. D., Frauenfeld, O. W., Nair, U., and Fall, S.: Land cover changes and their biogeophysical effects on climate, International Journal of Climatology, 34, 929–953, doi:10.1002/joc.3736, 2014.

Meng, Q., Latif, M., Park, W., Keenlyside, N. S., Semenov, V. A., and Martin, T.: Twentieth century Walker Circulation change: Data analysis and model experiments, Climate dynamics, 38, 1757–1773, doi:10.1007/s00382-011-1047-8, 2012.

Misra, V., Michael, J.-P., Boyles, R., Chassignet, E. P., Griffin, M., and O'Brien, J. J.: Reconciling the spatial distribution of the surface temperature trends in the southeastern United States, Journal of Climate, 25, 3610–3618, doi:10.1175/JCLI-D-11-00170.1, 2012.

Puma, M. J. and Cook, B. I.: Effects of irrigation on global climate during the 20th century, Journal of Geophysical Research, 115, D16 120, doi:10.1029/2010JD014122, 2010.

Rayner, N. A., Parker, D. E., Horton, E. B., Folland, C. K., Alexander, L. V., Rowell, D. P., Kent, E. C., and Kaplan, A.: Global analyses of sea surface temperature, sea ice, and night marine air temperature since the late nineteenth century, Journal of Geophysical Research, 108, 4407, doi:10.1029/2002JD002670, 2003.

Schmidt, G. A., Kelley, M., Nazarenko, L., Ruedy, R., Russell, G. L., Aleinov, I., Bauer, M., Bauer, S. E., Bhat, M. K., Bleck, R., Canuto, V., Chen, Y.-H., Cheng, Y., Clune, T. L., Del Genio, A., de Fainchtein, R., Faluvegi, G., Hansen, J. E., Healy, R. J., Kiang, N. Y., Koch, D., Lacis, A. A., LeGrande, A. N., Lerner, J., Lo, K. K., Matthews, E. E., Menon, S., Miller, R. L., Oinas, V., Oloso, A. O., Perlwitz, J. P., Puma, M. J., Putman, W. M., Rind, D., Romanou, A., Sato, M., Shindell, D. T., Sun, S., Syed, R. A., Tausnev, N., Tsigaridis, K., Unger, N., Voulgarakis, A., Yao, M.-S., and Zhang, J.: Configuration and assessment of the GISS ModelE2 contributions to the CMIP5 archive, Journal of Advances in Modeling Earth Systems, 6, 141–184, doi:10.1002/2013MS000265, http://dx.doi.org/10.1002/2013MS000265, 2014.

Shaman, J. and Tziperman, E.: The effect of ENSO on Tibetan plateau snow depth: A stationary wave teleconnection mechanism and implications for the south Asian monsoons, Journal of Climate, 18, 2067–2079, 2005.

Shukla, S. P., Puma, M. J., and Cook, B. I.: The response of the South Asian Summer Monsoon circulation to intensified irrigation in global climate model simulations, Climate Dynamics, 42, 21–36, 2014.

Swann, A. L., Fung, I. Y., Levis, S., Bonan, G. B., and Doney, S. C.: Changes in Arctic vegetation amplify high-latitude warming through the greenhouse effect, Proceedings of the National Academy of Sciences, 107, 1295–1300, doi:10.1073/pnas.0913846107, 2010.

Wada, Y., Wisser, D., Eisner, S., Flörke, M., Gerten, D., Haddeland, I., Hanasaki, N., Masaki, Y., Portmann, F. T., Stacke, T., et al.: Multimodel projections and uncertainties of irrigation water demand under climate change, Geophysical Research Letters, 40, 4626–4632, 2013.

Wisser, D., Fekete, B. M., Vörösmarty, C. J., and Schumann, A. H.: Reconstructing 20th century global hydrography: a contribution to the Global Terrestrial Network- Hydrology (GTN-H), Hydrology and Earth System Science, 14, 1–24, doi:10.5194/hess-14-1-2010, 2010.

Wu, R. and Kirtman, B. P.: Impacts of the Indian Ocean on the Indian summer monsoon – ENSO relationship, Journal of Climate, 17, 3037–3054, doi:10.1175/1520-0442(2004)017<3037:IOTIOO>2.0.CO;2, 2004.